Received: 29 September 2017 | Accepted: 3 January 2018

DOI: 10.1111/1365-2745.12973

LINKING ORGANISMAL FUNCTIONS, LIFE HISTORY STRATEGIES AND POPULATION PERFORMANCE

Journal of Ecology | BRITISH ECOLOGICAL SOCIETY

Microenvironment and functional-trait context dependence predict alpine plant community dynamics

Benjamin Blonder[1,2,3,4] | Rozalia E. Kapas[2,3] | Rebecca M. Dalton[3,5] | Bente J. Graae[2,3] | Jacob M. Heiling[3,6] | Øystein H. Opedal[3,7]

[1]Environmental Change Institute, School of Geography and the Environment, University of Oxford, Oxford, UK; [2]Department of Biology, Norwegian University of Science and Technology (NTNU), Trondheim, Norway; [3]Rocky Mountain Biological Laboratory, Crested Butte, CO, USA; [4]School of Life Sciences, Arizona State University, Tempe, AZ, USA; [5]University Program in Ecology, Nicholas School of the Environment, Duke University, Durham, NC, USA; [6]Department of Applied Ecology, North Carolina State University, David Clark Labs, Raleigh, NC, USA and [7]Department of Biology, Centre for Biodiversity Dynamics, Norwegian University of Science and Technology (NTNU), Trondheim, Norway

Correspondence
Benjamin Blonder
Email: bblonder@gmail.com

Funding information
Norwegian Research Council, Grant/Award Number: KLIMAFORSK #250233 and 223257; Natural Environment Research Council, Grant/Award Number: NE/M019160/

Handling Editor: Roberto Salguero-Gómez

Abstract

1. Predicting the structure and dynamics of communities is difficult. Approaches linking functional traits to niche boundaries, species co-occurrence and demography are promising, but have so far had limited success.
2. We hypothesized that predictability in community ecology could be improved by incorporating more accurate measures of fine-scale environmental heterogeneity and the context-dependent function of traits. We tested these hypotheses using long term whole-community demography data from an alpine plant community in Colorado.
3. Species distributions along microenvironmental gradients covaried with traits important for below-ground processes. Positive associations between species distributions across life stages could not be explained by abiotic microenvironment alone, consistent with facilitative processes. Rates of growth, survival, fecundity and recruitment were predicted by the direct and interactive effects of trait, microenvironment, macroenvironment and neighbourhood axes.
4. *Synthesis*. Context-dependent interactions between multiple traits and microenvironmental axes are needed to predict fine-scale community structure and dynamics.

KEYWORDS

Below-ground processes, biotic interactions, demography, environmental filtering, facilitation, functional trait, interaction network, microclimate

1 | INTRODUCTION

A long-standing challenge for ecological theory has been to predict the structure and dynamics of plant communities from basic principles (Keddy, 1992; Weiher et al., 2011). At large spatial scales, species assemblages can be predicted by relatively simple models of species sorting and niches (von Humboldt & Bonpland, 1807 (tr. 2009); Whittaker, 1967), but this becomes challenging at finer scales. Biotic interactions or neutral processes may play increasingly important roles (McGill, 2010), leading to the apparently stochastic loss and gain of species, and thus reduced predictability of community structure (Vellend, 2010). Consequently, community ecology

© 2018 The Authors. Journal of Ecology
© 2018 British Ecological Society

is often perceived as a "mess" (Lawton, 1999), with many researchers abandoning fine-scale prediction. However, delineating when prediction is possible is a necessary prerequisite for determining if investing in collecting sufficient data for predictive modelling is worthwhile, e.g. for climate change, invasion and land management applications (Blonder et al., 2017).

Here, we hypothesize that much of the apparent stochasticity in community structure and dynamics is due to deterministic environmental heterogeneity at fine spatial scales (Butterfield, 2009; Ellsworth & Reich, 1992; Stark, Lehman, Crawford, Enquist, & Blonder, 2017). Many studies have identified edaphic and microclimatic variables driving species distributions (Asner, Knapp, Anderson, Martin, & Vaughn, 2016; Kobe, 1999; Simpson, Richardson, & Laughlin, 2016) that often vary more within a few metres at a single site than the mean values across sites separated by kilometers (Opedal, Armbruster, & Graae, 2015; Scherrer & Körner, 2011; Stark et al., 2017). Thus, microenvironmental heterogeneity could impact both current community structure and community dynamics over time.

We also hypothesize that much of the variation in species' responses to microclimatic variation is mediated by the context-dependent function of traits. A long research program has argued for environmental sensitivity of functional traits which in turn affect performance and ultimately fitness (Arnold, 1983). These linkages are often explored in terms of direct effects of each variable, although interactive effects may be more important. Thus, incorporating interactions between functional traits and the microenvironment may improve predictability of communities.

Trait-mediated effects on community dynamics could arise in several ways. First, functional traits may influence the realized niche boundaries or physiological tolerances of species (Violle & Jiang, 2009), as in models using "response traits" (Lavorel & Garnier, 2002) to predict abundance based on trait-environment relationships along gradients (Laughlin, Joshi, van Bodegom, Bastow, & Fulé, 2012; Shipley et al., 2016). Consequently, we expect species distributions across environmental gradients to be correlated with species' functional traits. At regional and global scales, some studies have shown that realized niche boundaries for temperature and precipitation are linked to commonly measured traits (Laughlin et al., 2012), while others have failed to detect such relationships (Moles et al., 2014).

Second, functional traits could scale up to influence biotic interactions, and thus species co-occurrence patterns (Morueta-Holme et al., 2016; Soliveres et al., 2014). Individual plants may modulate their microenvironment, driving facilitation (Schöb, Butterfield, & Pugnaire, 2012) and/or competition (Falster, Brännström, Westoby, & Dieckmann, 2017), leading to species with either shared or disjoint spatial distributions. Consideration of these effects could thus increase predictability if their direction and magnitude depend systematically on functional traits of the interacting species. Existing work suggests that such pairwise effects may arise either from trait differences (more similar species compete more strongly) (Herben & Goldberg, 2014; Webb, Ackerly, McPeek, & Donoghue, 2002; Wilson, 2007) or trait hierarchies (species with more extreme trait values compete more strongly) (Kunstler et al., 2012; Mayfield & Levine, 2010).

Third, functional traits could influence the vital rates of species that in turn determine community dynamics (Adler et al., 2014; Funk & Wolf, 2016; Kunstler et al., 2012, 2016; Visser et al., 2016; Wright et al., 2010). While some traits and environments may uniformly modulate fitness, most may be functional only in certain biotic or abiotic contexts (==REF to editorial==). In other words, species' vital rates could be correlated with traits, microenvironment, trait by microenvironment interactions, and the traits and microenvironment of their neighbours. It has been difficult to elucidate mechanisms underlying variation in vital rates, primarily due to the difficulty of obtaining detailed long-term datasets from natural plant communities. So far, empirical studies linking vital rates to traits have largely been restricted to direct effects, independent of context, e.g. Kunstler et al. (2012)—but see Baraloto, Goldberg, and Bonal (2005).

To explore whether functional traits and detailed microenvironmental data could improve the predictability of fine-scale community structure and dynamics, we use a dataset for alpine plants co-occurring on permanent plots in the Colorado Rocky Mountains. Over four annual censuses, we mapped every individual plant (seedlings and adults) in each plot and measured growth, survival, fecundity and recruitment of every individual. We paired this demographic dataset with multiple below-ground and above-ground microenvironment variables measured at meter resolution within each plot. We also integrated below-ground and above-ground functional trait data for each species representative of key ecological strategy axes. We then used a set of regression analyses to determine whether interactions between traits and microenvironment could predict fine-scale species distributions, co-occurrence metrics, and/or vital rates.

2 | MATERIALS AND METHODS

2.1 | Site description

We established a long-term alpine research site in the Gunnison National Forest in Colorado (38.978725°N, 107.042104°W) (Figure 1a). The site is located on a southeast-facing ridgeline at *c.* 3,540 m above sea level and is on a *c.* 20% slope (Figure 1b). The substrate is Mancos shale (Upper Cretaceous) at the downslope end, with weak gradation at the upslope end to quartz monzonite porphyry (Upper Eocene). On both rock types there is a surface layer of loose weathered gravel, with bedrock occurring at depths of no more than 5–10 cm. The site is primarily barren, with *c.* 0–10% cover by perennial graminoids, forbs and woody mat plants during the short summer growing season. Snow is deposited on the site normally beginning in October, with melting between June and July. Because the site is on a ridgeline, avalanches are rare, though strong west-to-east winds are common.

In the summer of 2014, we established a set of fifty 2 × 2 m permanent plots arranged in a grid 5 plots wide by 10 plots long, following the main ridge axis (*c.* 40° heading), with a 2 × 2 m buffer

between each plot. The overall site covers an 18 × 38 m rectangular area (Figure 1c).

2.2 | Census data

Each year from 2014 to 2017 ($n = 4$), we censused each permanent plot when vegetative growth was complete and flowering was taking place, typically in late July or early August. Every individual plant (including seedlings) was located to the nearest centimetre in Cartesian coordinates relative to the lower left corner of each plot, and given a permanent aluminium tag nailed into nearby substrate. Species identities were determined based on a set of voucher specimens stored at the Rocky Mountain Biological Laboratory ("RMBL") Herbarium. One species could not be identified (a single seedling that died in the same year) and was named "*Indet indet*".

At each census, we recorded a set of demographic parameters for each individual. We recorded size as maximum length and maximum height of vegetative parts (cm) using a ruler. Delineating individuals was not always possible, e.g. for grasses and sedges. Stems separated by more than 3 cm at ground height were assumed to represent different individuals, except in cases of large mat plants with branches clearly connected below ground level. We recorded whether individuals were new recruits, either as seedlings (with cotyledons present) or as vegetative/clonal propagation (with no

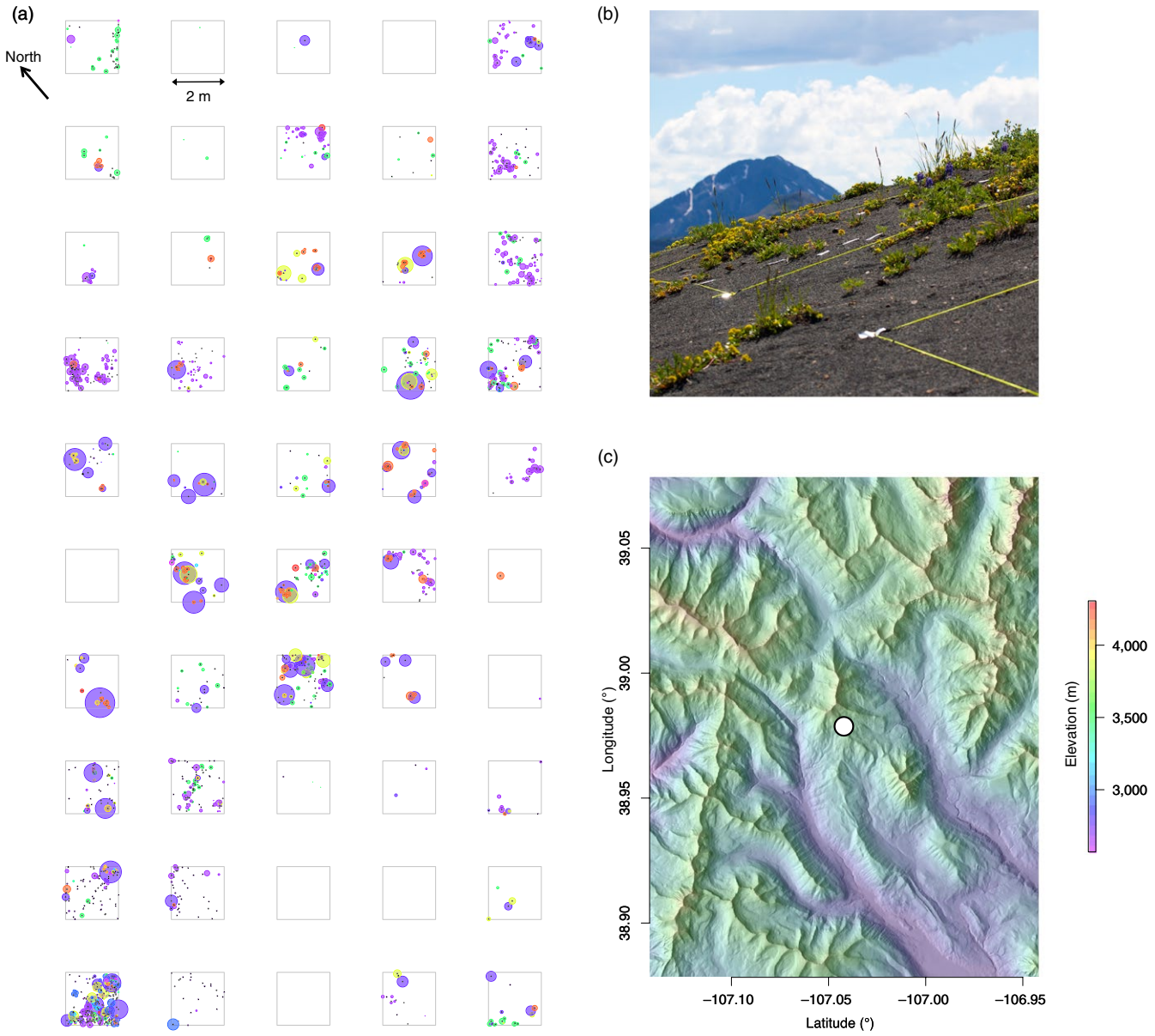

FIGURE 1 The study site is located on a ridgeline in the Rocky Mountains of southwestern Colorado. (a) Maps of individuals across plots in 2015. Circles represent vegetative lengths of each individual and are coloured by species. Individuals that recruited are shown with a +, that died, with a ×; that flowered, with a △. A zoomed version of this panel, with four years of data and with legend is available as Figure S1. (b) Photograph of 2 × 2 m plots, looking westward. (c) Relief map of the area, with the site location shown as a circle [Colour figure can be viewed at wileyonlinelibrary.com]

cotyledons present, and possibly still connected to a parent). We estimated fecundity as the number of mature floral structures per individual (e.g. number of flowers for *Viola praemorsa*, number of inflorescences for Asteraceae, number of spikelets for Poaceae and number of spikes for *Lupinus argenteus*). Individuals that were censused in 1 year but that failed to produce above-ground growth in a subsequent year were scored as either dormant or dead. If individuals failed to produce above-ground growth for more than two consecutive years, we assumed they were dead and removed their tag. Seedlings that germinated and then withered in the same year were scored as dead after a single year.

2.3 | Microenvironmental data

To explore spatially variable microenvironmental drivers, we mapped a large set of below-ground and above-ground factors describing physiography and disturbance. Field measurements were obtained at each corner of each plot (2 m resolution) and then interpolated within each plot to produce a map at 10 cm resolution using ordinary kriging.

We measured substrate surface temperature (°C) using dataloggers (iButton Thermochron DS1921G, Maxim) wrapped in gray duct tape to match the albedo of the substrate (Stark et al., 2017) and left at surface level. Loggers recorded data every 20 min between 13 July and 10 August 2016, and we used the median value per logger in subsequent analyses.

We measured local slope (m/m) using a clinometer and elevation by integrating clinometer measurements across the site. We then estimated aspect (°) based on these elevation data. We measured a proxy for disturbance intensity (m) as distance (based on Euclidean distance transformation, Zeller, McGarigal, & Whiteley, 2012) from a small animal trail that historically traversed the eastern side of the site.

Several days after a rain event in July 2015 we measured shallow soil moisture (g/g) at 3.8 cm depth using a FieldScout TDR 100 probe (Spectrum Technologies) inserted into the upper soil layer. We also measured deep soil moisture (g/g) volumetrically on cores taken at up to 10 cm depth (depending on bedrock stratigraphy) several days after a rain event in July 2016. The soil samples were dried at 150°C for 4 hr, after which soil sieves were used to quantify soil texture as dry mass fractions (g/g) of particles ≥4 mm, ≥2 mm, ≥1 mm, ≥0.5 mm and ≤0.5 mm. We then measured soil chemical properties for a subset of 23 of the soil samples that evenly gridded the site. Bulk samples were ground to powder and measured for concentrations (ppm) of copper, iron, potassium, manganese, phosphorus, zinc, total nitrates/nitrogen (%), organic matter content (%), pH, and electrical conductivity (mmho/cm). Analyses were conducted by the Colorado State University Soil, Water, and Plant Testing Lab.

We measured a proxy for hardness and fracturability of the soil as soil penetration energy density (MJ/m^3), in July 2015. Values were calculated as the gravitational potential energy required to hammer a nail (16-penny size) flush into the substrate, divided by the volume of the nail.

2.4 | Macroenvironmental data

To explore temporally variable drivers of community structure, we obtained annual climate data from 2013 to 2017 from the nearby (4.5 km distance) "Billy Barr" weather station, part of Environmental Protection Agency site "GTH161". For each year we calculated total precipitation from January through July (i.e. the majority of the snowpack water and summer rain).

2.5 | Functional trait data

To characterize species' ecological strategies, we measured a set of below-ground and above-ground metrics. To avoid disturbance of the permanent plots, individuals of each species were selected from locations immediately adjacent to the permanent plots. For each species, we excavated 3–5 whole individual plants and root systems, and stored them in moist paper towels for rehydration in a cooler or refrigerator for no more than 24 hr before processing. We measured (in cm) above-ground maximum vegetative height, and maximum width, maximum root depth, maximum root length, and maximum extent of rooting. We floated a sample of fine (<2 mm diameter) roots in water and obtained a high-resolution digital image with a camera (Canon, T2i, 17–40 mm f/4L lens). We then hand-traced all roots in ImageJ (NIH) using the SmartRoot plugin and obtained estimates of total root length (mm), total root volume and mean root cross-sectional area (cm^2). We dried these fine roots for 1 week at 65°C and measured their dry mass, then divided root length by dry mass to estimate specific root length (mm/g) and divided dry mass by volume to obtain root tissue density (g/cm^3).

We clipped a small (*c.* 0.5 g) subsample of each root system into 2-cm lengths, cleared it in a 10% KOH solution, stained it with a 0.01% trypan blue solution (Koske & Gemma, 1989), and mounted it on microscope slides. We estimated prevalence of arbuscular mycorrhizal fungi (AMF) (%), and dark-septate endophyte fungi (DSE) (%) using the magnified intercept method (McGonigle, Miller, Evans, Fairchild, & Swan, 1990) on a minimum of 50 root intersections.

We measured leaf traits for five leaves per individual: leaf lamina thickness (mm) using a micrometer (Tresna) and fresh leaf mass (g) using a balance. We obtained a digital image of each leaf (without petiole) using a scanner at 300 dpi resolution and estimated leaf area (cm^2) as well as leaf aspect ratio (ratio of major and minor axis lengths for an ellipse fitted to leaf silhouette). For compound leaves we included all leaflets and the rachis. We dried the leaves at 65°C for 1 week and measured their mass, to calculate specific leaf area (cm^2/g) and leaf dry matter content (g/g).

We separated excavated plants into reproductive structures, leaves, stems, coarse roots (>2 mm diameter) and fine roots (<2 mm diameter), weighed each tissue type before drying, and estimating biomass fractions of leaves, stems, coarse roots and fine roots (g/g) as well as root dry matter content and stem dry matter content (g/g).

For a separate set of three leaves from a non-harvested individual, we measured per-mass photosynthetic capacity (light-saturated photosynthetic rate) (μmol C g s^{-1}). Using a LiCor 6400XT we

measured leaves while attached to the plant, under controlled conditions at 1,500 μmol photosynthetically active radiation, 400 ppm CO_2, 25°C leaf temperature and ambient relative humidity (typically 20–60%). For species with leaves smaller than the instrument cuvette, we measured the total leaf projected area enclosed in each cuvette by scanning leaves in a digital scanner as above. For species with curled leaves (e.g. *Ivesia gordonii*), we multiplied leaf area by a scaling factor of two. We obtained an estimate of per-mass photosynthetic rate by multiplying raw per-area values by the area of the cuvette divided by the corrected leaf area and then further multiplying by the specific leaf area of these samples.

We measured leaf carbon concentration (g/g), leaf nitrogen concentration, leaf $\delta^{13}C$ and leaf $\delta^{15}N$ on ground dried leaf samples from the excavated plants using a PDZ Europa ANCA-GSL elemental analyser interfaced to a PDZ Europa 20-20 isotope ratio mass spectrometer (Sercon Ltd., Cheshire, UK) at the Stable Isotope Facility at the University of California Davis.

At the end of the 2015 growing season, we sampled 10 mature fruits from fertile individuals of each species. We dissected fruits, dried all seeds (number of seeds per fruit, mean $n = 29$, $SD = 25$), and separated apparently fertile from aborted seeds. We then measured relative seed set as the fraction of fertile seeds. We measured mean seed mass (mg) by weighing a bulk sample of seeds and dividing by the seed count.

2.6 | Data summarization

To summarize microenvironments, we obtained predicted values for all variables on the kriged grid spanning the site and conducted a principal components analysis (PCA) on these data after *z*-transforming each variable. We retained principal components with eigenvalues greater than unity, and obtained predicted scores along these components at 10 cm gridded resolution.

For realized niches, we scored species presence or absence at each point on the 10 cm grid ($n = 20{,}000$ grid cells), assuming that each individual was a circle with diameter equal to its maximum vegetative width in each year. We then obtained predicted microenvironment principal component scores at each grid point for which species were present. The median of this distribution represents the realized niche centroid.

To summarize vital rates, we defined recruitment events whenever a new plant established as either a seedling or vegetative propagule in a single year, growth rate as the change in vegetative length across a pair of years, mortality events whenever an individual died in a given year, and fecundity events as the number of floral structures produced in a single year (acknowledging that not all floral structures have equivalent effects on seed production and germination).

To summarize functional traits, we calculated species means. A small number of missing observations (68/540) were gap-filled using multiple imputation by chained equations (White, Royston, & Wood, 2011). We conducted a PCA on trait data after *z*-transforming variables, retained principal components with eigenvalues greater than unity (Legendre & Legendre, 2012), and obtained predicted scores along these components for each species.

To summarize species-level trait neighbourhoods, we calculated two metrics of pairwise trait differentiation for species mean functional trait principal component X and species m and n: absolute difference ($|X_m - X_n|$) and hierarchical difference (0, if $X_m < X_n$; $X_m - X_n$, otherwise).

To summarize individual-level trait neighbourhoods, we defined the crowding coefficient for each focal plant j as a sum over all other non-focal individuals k whose maximum vegetative sizes s_k yielded circles of that diameter within 50 cm of the equivalent circle of the focal plant as $\sum_k s_k e^{-d_{jk}/\delta}$, where $d_{jk}$is the distance between individuals' positions and δ is a decay constant, set to 20 cm. The value of the decay constant was chosen to roughly match the average below-ground root spreading distance in our trait data and that of others (Chu & Adler, 2015). We calculated this coefficient for both intra- and interspecific neighbours. We defined the mean trait difference for each individual j, as a size-weighted mean trait value around each focal individual minus the value of the focal individual's trait T, as $\sum_k s_k T_k / \sum_k s_k - T_k$, using the same 50 cm radius. We defined the mean trait hierarchy value for each individual j, as a size-weighted mean trait value around each focal individual as $\sum_k s_k T_k / \sum_k s_k$ (using the same 50 cm radius) if this value was greater than the focal species' trait value T_k and 0 otherwise. These estimates of trait difference and trait hierarchy do include individual-level data of s_k, but necessarily use species-mean values of T_k. While allometric scaling of trait values with plant size could potentially provide better individual-level trait estimates, empirical size-trait relationships were generally weak (data not shown).

2.7 | Statistical analysis

To assess covariation between traits and species' realized niches, we used linear mixed models to determine whether niche centroids varied with functional-trait principal components at the species level over years ($n = 67$). We included fixed effects for trait principal components and a random intercept for year.

To estimate trait effects on pairwise co-occurrence, we first assembled a matrix with rows corresponding to grid points and columns corresponding to the presence/absence of a vital rate event for each species across all 4 years of the study, and also for the predicted microenvironment principal component scores. We then calculated the partial correlation matrix of this matrix using a shrinkage estimator (Morueta-Holme et al., 2016), setting weak coefficients with absolute magnitude <0.1 to 0. These partial correlations are direct associations between species' vital rates that cannot be explained by shared microenvironment requirements, and can tentatively be interpreted as biotic interactions (given the number of abiotic variables they are known not to represent). Coefficients closer to +1 indicate facilitation, coefficients closer to −1 indicate competition, and coefficients closer to 0 indicate no biotic processes. We then used linear regression to determine whether partial correlations between vital rate events could be predicted by the species-level trait neighbourhoods.

To estimate trait and microenvironment effects on vital rates, we built linear mixed models of vital rates, treating recruitment and mortality as binomial-family models with logit link functions, growth as a Gaussian-family model with identity link function, and fecundity as Poisson-family model with log link function. Models for growth, fecundity and survival were fit to the set of individual demographic events across all 4 years as replicates. Because we only observed successful rather than failed recruitments events, the model for recruitment was fit using a dataset constructed from the subset of observed recruitment events, paired to a set of pseudo-failed recruitment events located in random locations across the plots where no recruitment of the focal species was observed. The number of pseudo-failed recruitment events was chosen to match the number of successful recruitment events for each species within each year. For survival models, individuals that died before census in a given year (i.e. assigned a size of 0) were re-assigned their prior-year size (in order to prevent model under-identification while still using size as a fixed effect). The overall structure of the fixed effects in the full model took the form:

$$\begin{aligned}\text{Vital rate} \sim\ & \text{Size} + \text{Size}^2 + \left(\sum_{i=1}^{3} \text{Trait PC}_i\right) \\ & \times \left(\sum_{j=1}^{3} \text{Micro environment PC}_j + \text{Macro environment Precipitation} \right. \\ & \left. + \text{Macro environment Precipitation Prior}\right) \\ & \times \left(\text{Crowding Intraspecific} + \text{Crowding Interspecific} \right. \\ & + \sum_{k=1}^{3} \text{Trait Neighborhood Difference PC}_k \\ & \left. + \sum_{k=1}^{3} \text{Trait Neighborhood Hierarchy PC}_k\right)\end{aligned}$$

The model also included random intercept and size-dependent slope for each species, reflecting the hierarchical structure of the data. The random slope for size was omitted for the recruitment model because propagule size would always be 0 or missing for a failed recruitment event. We did not include random intercepts for year (as it had few levels, and was correlated with the macroclimate data) or for plot (as it was correlated with the microenvironmental data). Only three principal components were included for each type of variable to limit the total number of fixed effects estimated (n = 218). All predictors were z-transformed before analysis to enable interpretation of regression coefficients as effect strengths in units of standard deviations.

For the mixed models we reported standardized coefficients for fixed effects as the mean coefficient estimate, approximate p-values using Type III ANOVA with Wald chi-square tests, and an overall model marginal or conditional R^2 as the sum of the fraction of variance explained by the fixed or fixed + random effects (Nakagawa & Schielzeth, 2013).

We conducted all analyses in R 3.3.3. Multiple imputation was performed using the *MICE* package. Spatial analyses were conducted using the *RASTER* and *SP* packages. Partial correlations were estimated with the *CORPCOR* package. Mixed models were built and evaluated using the *LME4*, *PIECEWISESEM*, and *CAR* packages. All data (microenvironment, traits, censuses and vital rates) are deposited in the Dryad repository (Blonder, 2018).

3 | RESULTS

3.1 | Patterns and trends

Permanent plots contained a mean of n = 40 (56 *SD*, max. 442) individuals of mean n = 6 (3 *SD*, max. 15) species (Figure 1c). Over 4 years, a total of 4,290 growth events, 1,422 mortality events, 1,464 recruitment events, and 1,691 fecundity events were recorded across 18 species (Figures S1 and S2).

The microenvironment varied extensively across plots (Figure 2a; Table S1). The 23 microenvironment variables had five principal component axes taking eigenvalues above unity (Figure 2b). Variation in the first axis (35% of the variance) described a gradient of moister, more fine-textured soils, with higher concentrations of manganese, phosphorus and nitrates/nitrogen, and lower pH and potassium concentrations (absolute loadings >0.25) (Figure 2c). Variation in the second axis (23% of the variance) described greater disturbance, and higher soil organic matter, electrical conductivity, and iron and copper concentrations, as well as lower soil penetration energy density (Figure 2d).

The macroenvironment at the site also varied across years (Table S2), with 2016 being drier, 2015 being wetter and 2014 and 2017 being closer to average.

Functional traits of species present at the site varied along multiple principal component axes (Figure 3a). The 30 original traits loaded onto 10 axes taking eigenvalues above unity (Figure 3b; Table S3). Variation in the first axis (19% of the variance) corresponded to larger size, as well as lower stem biomass fraction, and shorter root length (absolute loadings > 0.25) (Figure 3c). Variation in the second axis (17% of the variance) corresponded to more extensive and thicker roots, as well as lower stem and leaf dry matter content and lower specific root length (Figure 3d).

3.2 | Realized niches

We found that species occupied different portions of the microenvironmental space at the study site along the leading principal component axes (Figure 4a). Most species occupied a core central region in the microenvironmental space, but several species occupied

FIGURE 2 (a) Spatial variation in microenvironment axes across plots. Variables are z-transformed, with bluer colours indicating values below average and redder colours indicating values above average (note some variables have skewed distributions). (b) Biplot of principal components analysis of all microenvironment variables across all grid cells. Leading principal component axes are shown in red with scores as gray points. (c) Screeplot of fractional variance explained by each of the leading axes. Only axes with eigenvalues >1 are shown. (d, e) Loadings for the first two principal component axes. Purple vertical lines indicate thresholds chosen for significance [Colour figure can be viewed at wileyonlinelibrary.com]

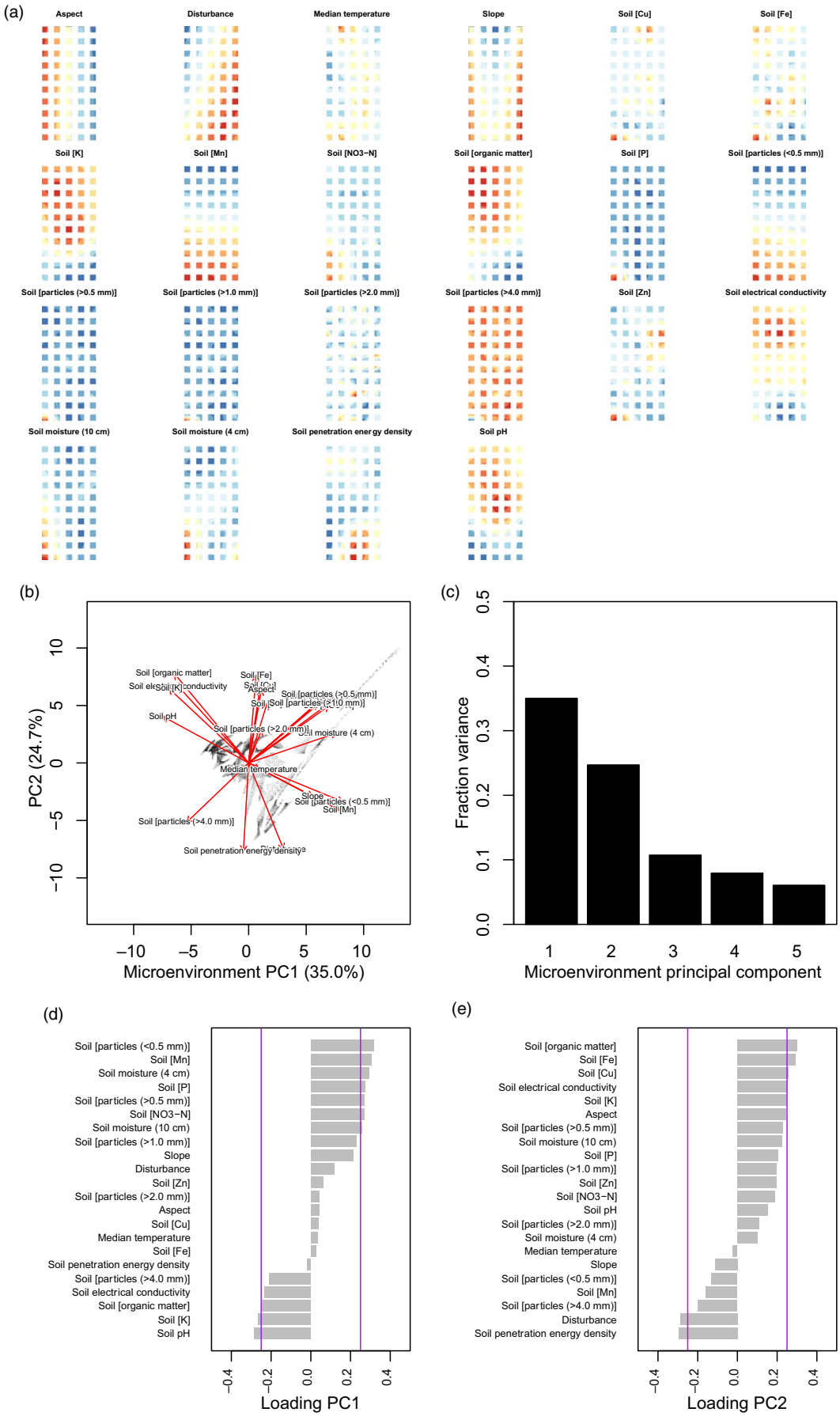
(a)
Aspect
Disturbance
Median temperature
Slope
Soil [Cu]
Soil [Fe]
Soil [K]
Soil [Mn]
Soil [NO3−N]
Soil [organic matter]
Soil [P]
Soil [particles (<0.5 mm)]
Soil [particles (>0.5 mm)]
Soil [particles (>1.0 mm)]
Soil [particles (>2.0 mm)]
Soil [particles (>4.0 mm)]
Soil [Zn]
Soil electrical conductivity
Soil moisture (10 cm)
Soil moisture (4 cm)
Soil penetration energy density
Soil pH
(b)
PC2 (24.7%)
Microenvironment PC1 (35.0%)
Soil [organic matter]
Soil [Fe]
Aspect
Soil [particles (>0.5 mm)]
Soil pH
Soil [particles (>2.0 mm)]
Soil moisture (4 cm)
Median temperature
Slope
Soil [particles (<0.5 mm)]
Soil [Mn]
Soil [particles (>4.0 mm)]
Soil penetration energy density
(c)
Fraction variance
Microenvironment principal component
(d)
Soil [particles (<0.5 mm)]
Soil [Mn]
Soil moisture (4 cm)
Soil [P]
Soil [particles (>0.5 mm)]
Soil [NO3−N]
Soil moisture (10 cm)
Soil [particles (>1.0 mm)]
Slope
Disturbance
Soil [Zn]
Soil [particles (>2.0 mm)]
Aspect
Soil [Cu]
Median temperature
Soil [Fe]
Soil penetration energy density
Soil [particles (>4.0 mm)]
Soil electrical conductivity
Soil [organic matter]
Soil [K]
Soil pH
Loading PC1
(e)
Soil [organic matter]
Soil [Fe]
Soil [Cu]
Soil electrical conductivity
Soil [K]
Aspect
Soil [particles (>0.5 mm)]
Soil moisture (10 cm)
Soil [P]
Soil [particles (>1.0 mm)]
Soil [Zn]
Soil [NO3−N]
Soil pH
Soil [particles (>2.0 mm)]
Soil moisture (4 cm)
Median temperature
Slope
Soil [particles (<0.5 mm)]
Soil [Mn]
Soil [particles (>4.0 mm)]
Disturbance
Soil penetration energy density
Loading PC2

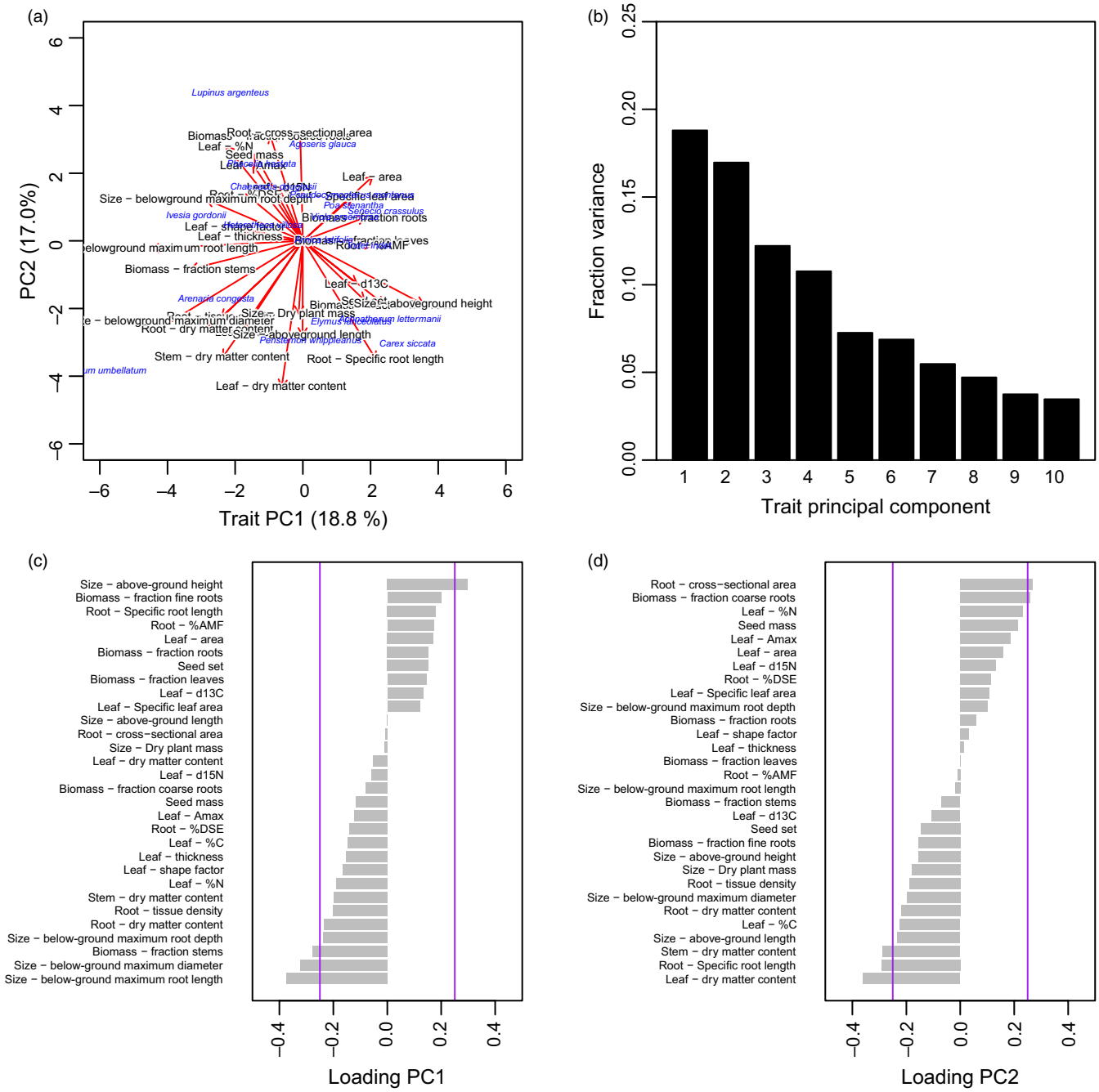

FIGURE 3 Variation in functional traits across all species in the plots. (a) Biplot of principal components analysis of trait values across all grid cells. Leading principal component axes are shown in red and species scores are shown in blue. (b) Screeplot of fractional variance explained by each of the leading principal component axes. Only axes with eigenvalues >1 are shown. (c, d) Loadings for the first two principal component axes. Purple vertical lines indicate thresholds chosen for significance [Colour figure can be viewed at wileyonlinelibrary.com]

outlying regions (e.g. *Viola praemorsa* and *Carex siccata*). Clear inter-annual variation was not visually evident.

A linear mixed model of the first microenvironment niche axis centroid including the first ten trait principal components as fixed effects revealed a close association between functional traits and species' fine-scale distributions. All axes were significant except for PC2 and PC3 ($p > .05$). The fixed effects jointly explained 76% of the variance in niche centroid value, with no increase in variance attributable to year effects. A similar model for the second micro-environment niche axis centroid had fixed effects explaining 81% of the variation.

Strong trait-environment covariation was readily evident in a scatterplot of the first two trait and microenvironment principal components (Figure 4b). These patterns are consistent with a leading (but only partial) role for finer textured and richer soils filtering for species with fast growth and long roots.

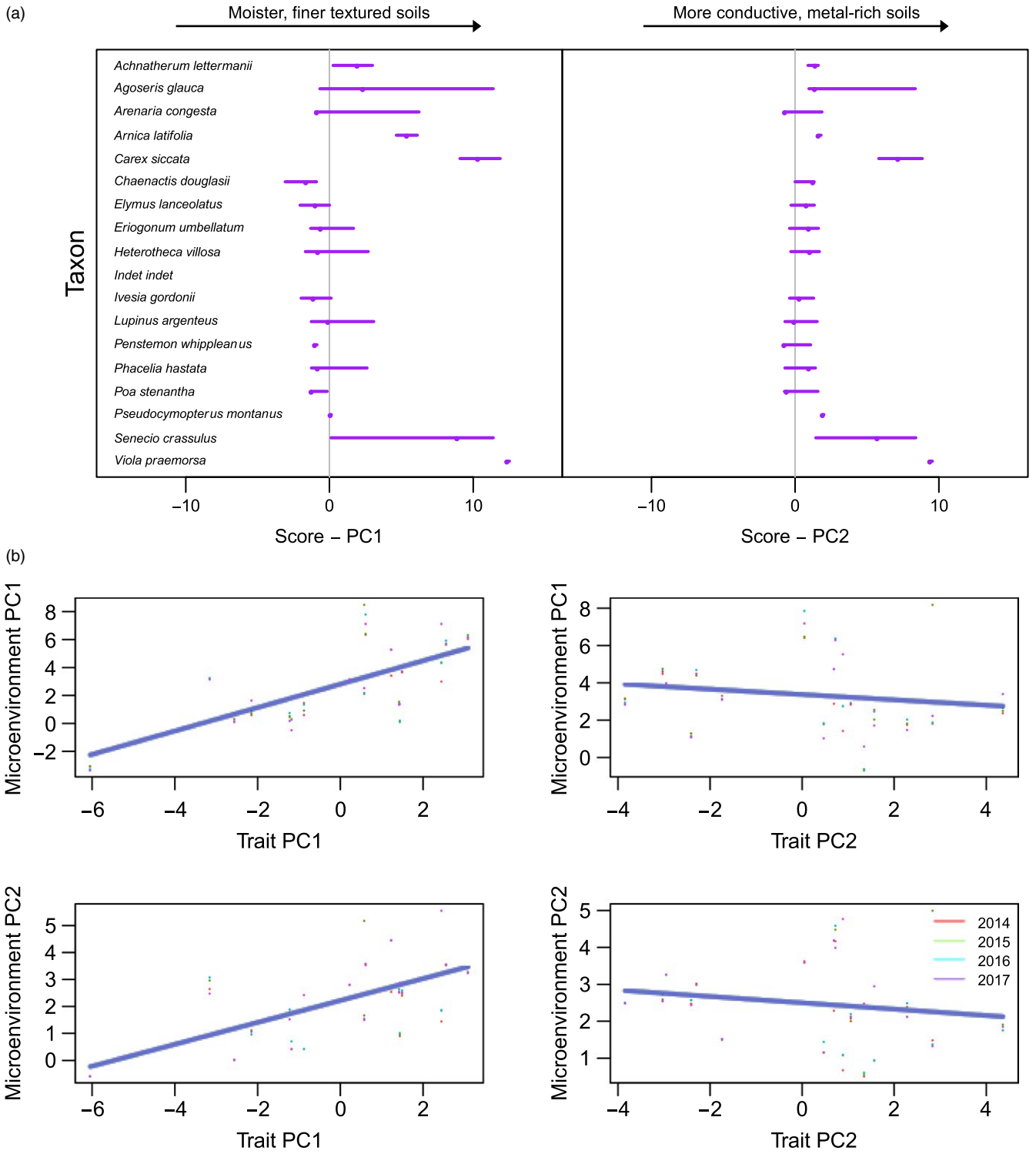

FIGURE 4 (a) Realized niches for all species using 2017 data, for the first and second microenvironment principal component axes. Points indicate median values, and line segments indicate inter-quartile range. Data are not shown for other years as they are very similar. (b) Partial residual plot for each the first two leading microenvironment principal components for the first two (of ten) leading trait principal components. Points indicate species-mean/environmental-median values, and regression lines indicate relationships fit for each year. Lines are overlapping due to the high inter-annual similarity [Colour figure can be viewed at wileyonlinelibrary.com]

3.3 | Co-occurrence patterns

The matrix of partial correlations among demographic events had a small fraction of non-zero coefficients (224/5112 possible links non-zero) (Figure 5a). Most of these coefficients were positive (170 positive vs. 64 negative), and positive coefficients were on average twice as large as negative coefficients. Inter- and intraspecific coefficients occurred at approximately equal frequencies and magnitudes

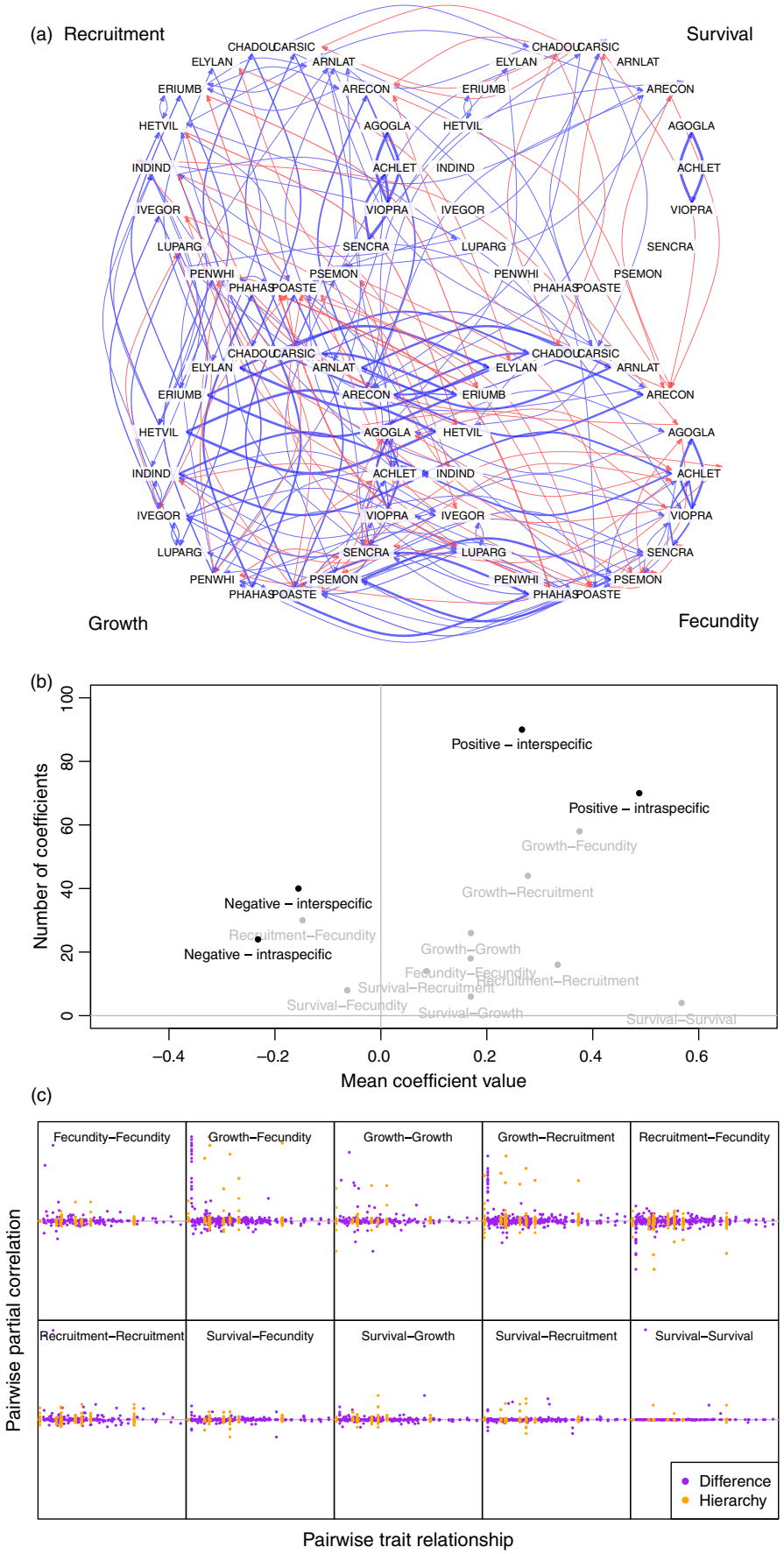

FIGURE 5 (a) Partial correlations between species' distributions for different vital rates, pooled across all four years. Edge strength indicates the direct effect of one taxon on another taxon's distribution after taking into account the effect of shared microenvironment and all other species' distributions. Blue edges indicate positive association; red, negative. Edge weight indicates magnitude of the partial correlation. Names are abbreviated using the first three letters of the genus and species for visual clarity. (b) Summary of the number and magnitude of partial correlation coefficients for interspecific vs. intraspecific and positive vs. negative categories (black) and among different vital rate pairs (gray). (c) Pairwise relationships between partial correlation coefficients and either trait hierarchies (orange) or differences (purple) for each vital rate pair [Colour figure can be viewed at wileyonlinelibrary.com]

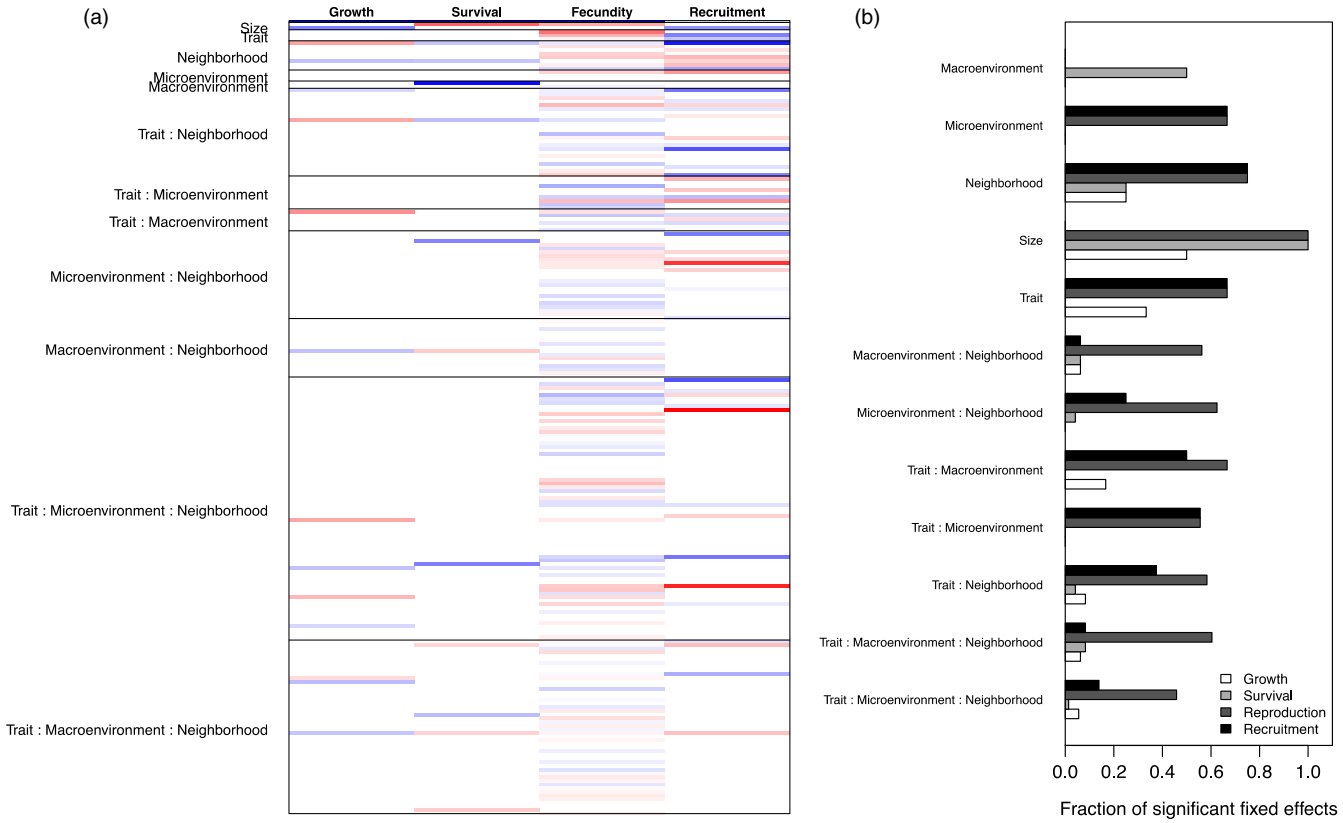

FIGURE 6 (a) Effect of different size, trait, microenvironment, macroenvironment and neighbourhood predictors on each vital rate. Grid colour indicates effect sign: bluer, more positive; redder, more negative. Effect sizes are scaled to unit range within each vital rate. Only statistically significant effects are coloured. (b) Summary of the fraction of variables within each category and vital rate that are statistically significant (normalized to the number of possible variables within each category) [Colour figure can be viewed at wileyonlinelibrary.com]

for both positive and negative coefficients. Recruitment-fecundity and survival-fecundity coefficients were consistently negative, while all others were generally positive. Most coefficients described growth-recruitment and growth-fecundity correlations (Figure 5b).

We then determined whether trait differences or hierarchies in either trait PC1 or trait PC2 predicted partial regression coefficients. There was no significant relationship between these four variables for the majority of the vital rate pairs ($p > .05$) (Figure 5c). Exceptions occurred for survival-growth ($R^2 = .04$), growth-recruitment ($R^2 = .12$), growth-fecundity ($R^2 = .15$) and recruitment-fecundity ($R^2 = .07$). The effect of trait distance PC1 and PC2, as well as trait hierarchy PC1 was significant for each of these models.

3.4 | Vital rates

Variation in all vital rates was associated with variation in a combination of size, functional trait, microenvironment, macroenvironment and neighbourhood variables, as well as interactions between these variable types (Figure 6a). Larger plants had uniformly greater growth, survival and fecundity rates. There were saturating (negative quadratic) effects of size on survival and fecundity, but not on growth.

The macroenvironment (prior precipitation) had a positive effect on survival, but no effect on growth, fecundity or recruitment. The microenvironment had only weak direct effects on vital rates except fecundity and recruitment, which increased along PC1 and decreased along PC2.

Functional traits of species affected vital rates in a variety of ways. Growth was higher for species with lower values of PC2. No trait axis directly affected survival. Fecundity was lower for higher values of PC2 and PC3. Recruitment was higher for higher values of PC1 and PC3.

Vital rates also depended on neighbour effects. Greater intraspecific crowding increased survival, fecundity and especially recruitment rates. Greater interspecific crowding also increased recruitment rates, but otherwise had no effect on other vital rates.

In all models, interactions between variables were more common than were main effects. For the growth model, 11 of 15 significant effects were interactions; for survival, 8 of 13; fecundity, 109 of 121, recruitment, 38 of 48. Across all types of interactions, significant interaction terms occurred approximately as frequently as significant main effect terms relative to the number of possible terms (24% [*SD* 40%] for interaction terms, 40% [*SD* 35%] for main effect terms, $p = .09$ [*t* test]) (Figure 6b). Significant interaction terms occurred among all variable types for all vital rates, and were approximately equally common across variable types. However, the sign and magnitude of each effect were heterogeneous across variable types, challenging interpretation.

Overall, all vital rates were well-explained by the variables we investigated. The model for growth explained 41% of variation from fixed effects alone, and 56% of variation when also including random

effects; for survival, 57% or 69%; for fecundity, 60% or 93%; and for recruitment, 97% or 97%.

4 | DISCUSSION

The structure and dynamics of an alpine plant community were closely tied to functional traits of the resident species and their microenvironments. This supports the central hypothesis that better incorporating these factors into models can improve the predictability of community ecology. In the following, we discuss several general conceptual implications of these findings that are relevant beyond the immediate study site.

We demonstrated strong microenvironmental control of species distributions. Importantly, the distribution of each species at this fine scale was strongly associated with species-mean functional trait values. These results suggest that much of the apparent stochasticity in fine-scale community structure is actually deterministic, and can be predicted based on trait-based species sorting. In particular, we found strong relationships between several below-ground-microenvironment variables and several below-ground traits, consistent with a growing recognition of the importance of below-ground processes (Laliberté, 2017).

The fine-scale distributions of species were not random, but depended both on environmental conditions and on the distribution of interacting species. Importantly, we showed that many species had spatial distributions that were strongly associated with other species' spatial distributions after accounting for the effects of shared microenvironmental requirements. These associations varied across species and vital rates, but were almost always positive. However, trait differences or trait hierarchies amongst species could rarely predict these associations. Thus, pairwise relationships between species' functional traits do not seem to provide insight into these co-occurrence patterns. Rather, traits seem to mediate occurrence patterns independently via the microenvironmental partitioning explored in the analyses above.

We showed that key vital rates are not stochastic, and are predictable from measurable parameters. The large component of variance attributed to random effects for fecundity suggests that other unmeasured factors differentially affect taxa, e.g. differential florivory, while other unmeasured or random factors, e.g. random vegetative herbivory may have caused the lower amount of variance explained for growth. Nevertheless, measured factors provide a mostly complete explanation for survival, fecundity and recruitment rates, and are also capable of explaining a large fraction of variation in growth rates.

However, predictability of vital rates did not arise solely from the main effects of each variable, but primarily from a wide set of interactions between variable types. With respect to vital rates, we showed that growth, survival, fecundity and recruitment could be predicted by a combination of functional traits, microenvironment, macroenvironment and neighbourhood effects (reflecting both trait-mediated and non-trait-mediated interactions). This finding suggests that the functional significance of traits is highly context dependent (==REF to editorial==). This might explain why partial correlation coefficients did not appear to be linked to traits after accounting for context-independent dependencies on environment. This may also explain why previous studies of co-occurrence also had limited success in explaining the observed patterns, e.g. Morueta-Holme et al. (2016). Additionally, the functional significance of each trait varied across vital rates. Relationships between traits and fitness are not necessarily simple, because traits had contrasting effects on different vital rates, and each of these effects had different context dependence. Thus, much of the variation in the importance of traits for demography, and ultimately fitness, may arise from inability to quantify trait interactions with neighbours, microenvironment and macroenvironment, e.g. Adler et al. (2014); Kunstler et al. (2016); Visser et al. (2016)—but see Lasky et al. (2015).

At our study site, facilitative processes appear to play a key role in structuring community dynamics. Evidence for facilitation arose from two sets of results: first, the high prevalence of positive associations between species' distributions that could not be explained by shared microenvironmental requirements, and second, the consistent positive effects of intraspecific (and sometimes interspecific) neighbourhood density on multiple vital rates. In contrast, we failed to detect strong evidence for competitive interactions in this system, consistent with the proposed greater importance of facilitation as stress increases (Callaway et al., 2002). This finding builds on a growing body of evidence that facilitation can be a strong mechanism structuring community dynamics, as seen in other desert and alpine communities (Butterfield, 2009; McIntire & Fajardo, 2014). This finding is important because many models of community dynamics assume that all interactions between species are purely competitive (e.g. Barabás, Michalska-Smith, & Allesina, 2016; Saavedra et al., 2017). Indeed, no existing trait-based models of species interactions yield facilitative interactions. For example, both the trait difference and trait hierarchy hypotheses we explored here yield only competitive outcomes. Better incorporating both positive and negative interactions into trait-based community ecology is an open challenge (Wright, Schnitzer, & Reich, 2014).

Environmental filtering and biotic interactions are often considered as independent processes driving community assembly (HilleRisLambers, Adler, Harpole, Levine, & Mayfield, 2012). However, this study suggests that, at fine scales, there may be no clear boundary between environmental filtering and biotic interactions (Soberón & Nakamura, 2009). When individuals modify their local microenvironments, e.g. by changing moisture, light, or thermal conditions, environmental and biotic-interaction processes are no longer independent, but rather interactive. We found evidence for trait—environment—neighbourhood interactions in vital rate regressions, as well as positive associations between individuals' fine-scale distributions, which are all consistent with this scenario. Additionally, this scenario would challenge community ecology frameworks that attempt to partition patterns into abiotic environmental filtering and biotic interaction components, e.g. (Swenson & Enquist, 2009; Webb et al., 2002).

The number of variables measured in this study required a level of effort likely beyond most practical situations in which predictions of community dynamics will be desired. It remains unclear how many (and which) variables must be measured before an acceptable level of predictability is achieved. It is possible that the high predictability obtained in this study is a result of model overfitting. On the other hand, the variables measured were largely mutually uncorrelated and could each be argued to have important functional roles. Much larger datasets might be able to resolve this question, but only at the cost of dramatically increased sampling effort. Even with the large number of demographic observations in this dataset, we were limited to modelling vital rates based on only the leading trait and microenvironment axes because of the rapid increase in the number of interaction terms with number of axes relative to the limited possible degrees of freedom in the data. Thus, a balance needs to be struck between large exploratory analyses such as this one, and the overly simplistic single-axis analyses that have largely characterized the field (==REF to editorial==). Rather, it may be useful to develop more mechanistic trait-based models of plant performance and population dynamics that could explore the implications of multidimensional trait variation on community structure and dynamics across contexts.

Several of our findings point to important roles for below-ground traits and microenvironment axes. Root traits like specific root length and maximum root length were associated with the leading axes of trait variation, and soil properties like penetration energy density, texture and pH were associated with the leading axes of microenvironment variation. Our study indicates that the predictability of community structure and dynamics is improved by the inclusion of below-ground variables (Laliberté, 2017; McCormack, Lavely, & Ma, 2014). The observed linkages among below-ground factors may generalize beyond alpine sites, and also extend other studies that have identified physiographic drivers of species distributions (Clark, Palmer, & Clark, 1999) to the community scale. Nevertheless, such measurements are time-intensive and often destructive (e.g. excavation of whole root systems). To circumvent these issues, there is a need for further developing below-ground trait databases (Freschet et al., 2017; Iversen et al., 2017) and fine-scale soil maps (Arrouays et al., 2014).

The main conclusion of this study is that the predictability of community structure and dynamics can be improved by accounting for multivariate microenvironmental heterogeneity, and the context-dependence of functional traits, especially below-ground. Incorporating microenvironment and context into trait-based ecology may provide more powerful approaches for understanding communities, though at greatly increased effort.

ACKNOWLEDGEMENTS

Lake Crawford, Sabastian Escobar, Guadalupe Flores, Kenny Helsen, Sean Michaletz, Jordan Stark, and Charlotte Wang provided assistance in the field. Vanessa Buzzard led stoichiometric analyses. Jeremiah Henning and Kenna Rewcastle led root staining work. David Inouye, Rosemary Smith, and James Thomson provided field vehicles. The project was supported by the Norwegian Research Council (KLIMAFORSK #250233) and the United Kingdom Natural Environment Research Council (NE/M019160/1). Ø.H.O. was supported by the Norwegian Research Council Center of Excellence funding scheme (223257). Research permits were coordinated by the Rocky Mountain Biological Laboratory and the United States Forest Service.

AUTHORS' CONTRIBUTIONS

B.B. designed the study. B.B., R.M.D., R.E.K. and Ø.H.O. planned and carried out fieldwork. B.B. analysed the data and wrote the manuscript with input from R.E.K., R.M.D., B.J.G., J.M.H. and Ø.H.O.

DATA ACCESSIBILITY

Data available from the Dryad Digital Repository: https://doi.org/10.5061/dryad.33410 (Blonder, 2018). We encourage prospective data users to contact us before embarking on any analyses.

ORCID

Benjamin Blonder http://orcid.org/0000-0002-5061-2385

REFERENCES

Adler, P. B., Salguero-Gómez, R., Compagnoni, A., Hsu, J. S., Ray-Mukherjee, J., Mbeau-Ache, C., & Franco, M. (2014). Functional traits explain variation in plant life history strategies. *Proceedings of the National Academy of Sciences of the United States of America*, *111*, 740–745. https://doi.org/10.1073/pnas.1315179111

Arnold, S. J. (1983). Morphology, performance and fitness. *American Zoologist*, *23*, 347–361. https://doi.org/10.1093/icb/23.2.347

Arrouays, D., Grundy, M. G., Hartemink, A. E., Hempel, J. W., Heuvelink, G. B. M., Hong, S. Y., … Zhang, G.-L. (2014). Chapter Three – GlobalSoilMap: Toward a fine-resolution global grid of soil properties. In D. L. Sparks (Ed.), *Advances in agronomy* (pp. 93–134). Cambridge, MA: Academic Press.

Asner, G. P., Knapp, D. E., Anderson, C. B., Martin, R. E., & Vaughn, N. (2016). Large-scale climatic and geophysical controls on the leaf economics spectrum. *Proceedings of the National Academy of Sciences of the United States of America*, *113*, E4043–E4051. https://doi.org/10.1073/pnas.1604863113

Barabás, G. J., Michalska-Smith, M., & Allesina, S. (2016). The effect of intra-and interspecific competition on coexistence in multispecies communities. *The American Naturalist*, *188*, E1–E12. https://doi.org/10.1086/686901

Baraloto, C., Goldberg, D. E., & Bonal, D. (2005). Performance trae-offs among tropical tree seedlings in contrasting microhabitats. *Ecology*, *86*, 2461–2472. https://doi.org/10.1890/04-1956

Blonder, B. (2018). Data from: Microenvironment and functional-trait context dependence predict alpine plant community dynamics. *Dryad Digital Repository*, https://doi.org/10.5061/dryad.33410

Blonder, B., Moulton, D. E., Blois, J., Enquist, B. J., Graae, B. J., Macias-Fauria, M., … Sandel, B. (2017). Predictability in community dynamics. *Ecology Letters*, *20*, 293–306. https://doi.org/10.1111/ele.12736

Butterfield, B. J. (2009). Effects of facilitation on community stability and dynamics: Synthesis and future directions. *Journal of Ecology*, *97*, 1192–1201. https://doi.org/10.1111/j.1365-2745.2009.01569.x

Callaway, R. M., Brooker, R. W., Choler, P., Kikvidze, Z., Lortie, C. J., Michalet, R., … Cook, B. J. (2002). Positive interactions among alpine plants increase with stress. *Nature*, *417*, 844–848. https://doi.org/10.1038/nature00812

Chu, C., & Adler, P. B. (2015). Large niche differences emerge at the recruitment stage to stabilize grassland coexistence. *Ecological Monographs*, *85*, 373–392. https://doi.org/10.1890/14-1741.1

Clark, D. B., Palmer, M. W., & Clark, D. A. (1999). Edaphic factors and the landscape-scale distributions of tropical rain forest trees. *Ecology*, *80*, 2662–2675. https://doi.org/10.1890/0012-9658(1999)080[2662:EFATLS]2.0.CO;2

Ellsworth, D., & Reich, P. (1992). Leaf mass per area, nitrogen content and photosynthetic carbon gain in Acer saccharum seedlings in contrasting forest light environments. *Functional Ecology*, *6*, 423–435. https://doi.org/10.2307/2389280

Falster, D. S., Brännström, Å., Westoby, M., & Dieckmann, U. (2017). Multitrait successional forest dynamics enable diverse competitive coexistence. *Proceedings of the National Academy of Sciences of the United States of America*, *114*, E2719–E2728. https://doi.org/10.1073/pnas.1610206114

Freschet, G. T., Valverde-Barrantes, O. J., Tucker, C. M., Craine, J. M., McCormack, M. L., Violle, C., … Iversen, C. M. (2017). Climate, soil and plant functional types as drivers of global fine–root trait variation. *Journal of Ecology*, *105*, 1182–1196. https://doi.org/10.1111/1365-2745.12769

Funk, J. L., & Wolf, A. A. (2016). Testing the trait-based community framework: Do functional traits predict competitive outcomes? *Ecology*, *97*, 2206–2211. https://doi.org/10.1002/ecy.1484

Herben, T., & Goldberg, D. E. (2014). Community assembly by limiting similarity vs. competitive hierarchies: Testing the consequences of dispersion of individual traits. *Journal of Ecology*, *102*, 156–166. https://doi.org/10.1111/1365-2745.12181

HilleRisLambers, J., Adler, P., Harpole, W., Levine, J., & Mayfield, M. (2012). Rethinking community assembly through the lens of coexistence theory. *Annual Review of Ecology, Evolution, and Systematics*, *43*, 227–248. https://doi.org/10.1146/annurev-ecolsys-110411-160411

Iversen, C. M., McCormack, M. L., Powell, A. S., Blackwood, C. B., Freschet, G. T., Kattge, J., … Valverde-Barrantes, O. J. (2017). A global Fine-Root Ecology Database to address below-ground challenges in plant ecology. *New Phytologist*, *215*, 15–26. https://doi.org/10.1111/nph.14486

Keddy, P. A. (1992). Assembly and response rules: Two goals for predictive community ecology. *Journal of Vegetation Science*, *3*, 157–164. https://doi.org/10.2307/3235676

Kobe, R. K. (1999). Light gradient partitioning among tropical tree species through differential seedling mortality and growth. *Ecology*, *80*, 187–201. https://doi.org/10.1890/0012-9658(1999)080[0187:LGPATT]2.0.CO;2

Koske, R. E., & Gemma, J. N. (1989). A modified procedure for staining roots to detect VA mycorrhizas. *Mycological Research*, *92*, 486–488. https://doi.org/10.1016/S0953-7562(89)80195-9

Kunstler, G., Falster, D., Coomes, D. A., Hui, F., Kooyman, R. M., Laughlin, D. C., … Wright, S. J. (2016). Plant functional traits have globally consistent effects on competition. *Nature*, *529*, 204–207. https://doi.org/10.1038/nature16476

Kunstler, G., Lavergne, S., Courbaud, B., Thuiller, W., Vieilledent, G., Zimmermann, N. E., … Coomes, D. A. (2012). Competitive interactions between forest trees are driven by species' trait hierarchy, not phylogenetic or functional similarity: Implications for forest community assembly. *Ecology Letters*, *15*, 831–840. https://doi.org/10.1111/j.1461-0248.2012.01803.x

Laliberté, E. (2017). Below-ground frontiers in trait-based plant ecology. *New Phytologist*, *213*, 1597–1603. https://doi.org/10.1111/nph.14247

Lasky, J. R., Bachelot, B., Muscarella, R., Schwartz, N., Forero-Montaña, J., Nytch, C. J., … Uriarte, M. (2015). Ontogenetic shifts in trait-mediated mechanisms of plant community assembly. *Ecology*, *96*, 2157–2169. https://doi.org/10.1890/14-1809.1

Laughlin, D. C., Joshi, C., van Bodegom, P. M., Bastow, Z. A., & Fulé, P. Z. (2012). A predictive model of community assembly that incorporates intraspecific trait variation. *Ecology Letters*, *15*, 1291–1299. https://doi.org/10.1111/j.1461-0248.2012.01852.x

Lavorel, S., & Garnier, E. (2002). Predicting changes in community composition and ecosystem functioning from plant traits: Revisiting the Holy Grail. *Functional Ecology*, *16*, 545–556. https://doi.org/10.1046/j.1365-2435.2002.00664.x

Lawton, J. H. (1999). Are there general laws in ecology? *Oikos*, *84*, 177–192. https://doi.org/10.2307/3546712

Legendre, P., & Legendre, L. F. (2012). *Numerical ecology*. Amsterdam, the Netherlands: Elsevier.

Mayfield, M. M., & Levine, J. M. (2010). Opposing effects of competitive exclusion on the phylogenetic structure of communities. *Ecology Letters*, *13*, 1085–1093. https://doi.org/10.1111/j.1461-0248.2010.01509.x

McCormack, M. L., Lavely, E., & Ma, Z. (2014). Fine-root and mycorrhizal traits help explain ecosystem processes and responses to global change. *New Phytologist*, *204*, 455–458. https://doi.org/10.1111/nph.13023

McGill, B. J. (2010). Matters of scale. *Science*, *328*, 575–576. https://doi.org/10.1126/science.1188528

McGonigle, T. P., Miller, M. H., Evans, D. G., Fairchild, G. L., & Swan, J. A. (1990). A new method which gives an objective measure of colonization of roots by vesicular—arbuscular mycorrhizal fungi. *New Phytologist*, *115*, 495–501. https://doi.org/10.1111/j.1469-8137.1990.tb00476.x

McIntire, E. J., & Fajardo, A. (2014). Facilitation as a ubiquitous driver of biodiversity. *New Phytologist*, *201*, 403–416. https://doi.org/10.1111/nph.12478

Moles, A. T., Perkins, S. E., Laffan, S. W., Flores-Moreno, H., Awasthy, M., Tindall, M. L., … Aarssen, L. W. (2014). Which is a better predictor of plant traits: Temperature or precipitation? *Journal of Vegetation Science*, *25*, 1167–1180. https://doi.org/10.1111/jvs.12190

Morueta-Holme, N., Blonder, B., Sandel, B., McGill, B. J., Peet, R. K., Ott, J. E., … Svenning, J. C. (2016). A network approach for inferring species associations from co-occurrence data. *Ecography*, *39*, 1139–1150. https://doi.org/10.1111/ecog.01892

Nakagawa, S., & Schielzeth, H. (2013). A general and simple method for obtaining R2 from generalized linear mixed-effects models. *Methods in Ecology and Evolution*, *4*, 133–142. https://doi.org/10.1111/j.2041-210x.2012.00261.x

Opedal, Ø. H., Armbruster, W. S., & Graae, B. J. (2015). Linking small-scale topography with microclimate, plant species diversity and intra-specific trait variation in an alpine landscape. *Plant Ecology & Diversity*, *8*, 305–315. https://doi.org/10.1080/17550874.2014.987330

Saavedra, S., Rohr, R. P., Bascompte, J., Godoy, O., Kraft, N. J., & Levine, J. M. (2017). A structural approach for understanding multispecies coexistence. *Ecological Monographs*, *87*, 470–486. https://doi.org/10.1002/ecm.1263.

Scherrer, D., & Körner, C. (2011). Topographically controlled thermal-habitat differentiation buffers alpine plant diversity against climate warming. *Journal of Biogeography*, *38*, 406–416. https://doi.org/10.1111/j.1365-2699.2010.02407.x

Schöb, C., Butterfield, B. J., & Pugnaire, F. I. (2012). Foundation species influence trait-based community assembly. *New Phytologist*, *196*, 824–834. https://doi.org/10.1111/j.1469-8137.2012.04306.x

Shipley, B., De Bello, F., Cornelissen, J. H. C., Laliberté, E., Laughlin, D. C., & Reich, P. B. (2016). Reinforcing loose foundation stones in trait-based plant ecology. *Oecologia*, *180*, 923–931. https://doi.org/10.1007/s00442-016-3549-x

Simpson, A. H., Richardson, S. J., & Laughlin, D. C. (2016). Soil–climate interactions explain variation in foliar, stem, root and reproductive traits across temperate forests. *Global Ecology and Biogeography*, *25*, 964–978. https://doi.org/10.1111/geb.12457

Soberón, J., & Nakamura, M. (2009). Niches and distributional areas: Concepts, methods, and assumptions. *Proceedings of the National Academy of Sciences of the United States of America*, *106*, 19644–19650. https://doi.org/10.1073/pnas.0901637106

Soliveres, S., Maestre, F. T., Bowker, M. A., Torices, R., Quero, J. L., García-Gómez, M., … Noumi, Z. (2014). Functional traits determine plant co-occurrence more than environment or evolutionary relatedness in global drylands. *Perspectives in Plant Ecology, Evolution and Systematics*, *16*, 164–173. https://doi.org/10.1016/j.ppees.2014.05.001

Stark, J., Lehman, R., Crawford, L., Enquist, B. J., & Blonder, B. (2017). Does environmental heterogeneity drive functional trait variation? A test in montane and alpine meadows. *Oikos*, *126*, 1650–1659. https://doi.org/10.1111/oik.04311

Swenson, N. G., & Enquist, B. J. (2009). Opposing assembly mechanisms in a Neotropical dry forest: Implications for phylogenetic and functional community ecology. *Ecology*, *90*, 2161–2170. https://doi.org/10.1890/08-1025.1

Vellend, M. (2010). Conceptual synthesis in community ecology. *The Quarterly Review of Biology*, *85*, 183–206. https://doi.org/10.1086/652373

Violle, C., & Jiang, L. (2009). Towards a trait-based quantification of species niche. *Journal of Plant Ecology*, *2*, 87–93. https://doi.org/10.1093/jpe/rtp007

Visser, M. D., Bruijning, M., Wright, S. J., Muller-Landau, H. C., Jongejans, E., Comita, L. S., & Kroon, H. (2016). Functional traits as predictors of vital rates across the life cycle of tropical trees. *Functional Ecology*, *30*, 168–180. https://doi.org/10.1111/1365-2435.12621

von Humboldt, A., & Bonpland, A. (1807 (tr. 2009)). *Essay on the geography of plants*. In S. T. Jackson (Ed.). Paris, France: University of Chicago Press.

Webb, C. O., Ackerly, D. D., McPeek, M. A., & Donoghue, M. J. (2002). Phylogenies and community ecology. *Annual Review of Ecology and Systematics*, *33*, 475–505. https://doi.org/10.1146/annurev.ecolsys.33.010802.150448

Weiher, E., Freund, D., Bunton, T., Stefanski, A., Lee, T., & Bentivenga, S. (2011). Advances, challenges and a developing synthesis of ecological community assembly theory. *Philosophical Transactions of the Royal Society of London B: Biological Sciences*, *366*, 2403–2413. https://doi.org/10.1098/rstb.2011.0056

White, I. R., Royston, P., & Wood, A. M. (2011). Multiple imputation using chained equations: Issues and guidance for practice. *Statistics in Medicine*, *30*, 377–399. https://doi.org/10.1002/sim.4067

Whittaker, R. H. (1967). Gradient analysis of vegetation. *Biological Reviews*, *42*, 207–264. https://doi.org/10.1111/j.1469-185X.1967.tb01419.x

Wilson, J. B. (2007). Trait-divergence assembly rules have been demonstrated: Limiting similarity lives! A reply to Grime. *Journal of Vegetation Science*, *18*, 451–452. https://doi.org/10.1111/j.1654-1103.2007.tb02557.x

Wright, S. J., Kitajima, K., Kraft, N. J., Reich, P. B., Wright, I. J., Bunker, D. E., … Díaz, S. (2010). Functional traits and the growth-mortality trade-off in tropical trees. *Ecology*, *91*, 3664–3674. https://doi.org/10.1890/09-2335.1

Wright, A., Schnitzer, S. A., & Reich, P. B. (2014). Living close to your neighbors: The importance of both competition and facilitation in plant communities. *Ecology*, *95*, 2213–2223. https://doi.org/10.1890/13-1855.1

Zeller, K. A., McGarigal, K., & Whiteley, A. R. (2012). Estimating landscape resistance to movement: A review. *Landscape Ecology*, *27*, 777–797. https://doi.org/10.1007/s10980-012-9737-0

SUPPORTING INFORMATION

Additional Supporting Information may be found online in the supporting information tab for this article.

How to cite this article: Blonder B, Kapas RE, Dalton RM, Graae BJ, Heiling JM, Opedal ØH. Microenvironment and functional-trait context dependence predict alpine plant community dynamics. *J Ecol*. 2018;106:1323–1337. https://doi.org/10.1111/1365-2745.12973